Conjugate Mixed Convection With Surface Radiation From a Vertical Plate With a Discrete Heat Source

C. Gururaja Rao
Research Scholar and Lecturer
Department of Mechanical Engineering,
Regional Engineering College,
Warangal—506 004 (AP), India

C. Balaji
Assistant Professor

S. P. Venkateshan
Professor
e-mail: spv46@usa.net

Heat Transfer and Thermal Power Laboratory,
Department of Mechanical Engineering,
Indian Institute of Technology Madras,
Chennai-600 036, India

The results of a numerical study of the problem of two-dimensional, steady, incompressible, conjugate, laminar, mixed convection with surface radiation from a vertical plate with a flush-mounted discrete heat source are reported. The governing equations, written in vorticity-stream function form, are solved using a finite-volume based finite difference method. A hybrid grid system has been employed for discretization of the computational domain. The effects of (i) the magnitude and location of the heat source, (ii) the material and surface properties of the plate, and (iii) the free-stream velocity on both heat transfer and fluid flow have been studied. Based on a large set of (more than 550) numerical data, correlations have been developed for maximum and average non-dimensional plate temperatures and mean friction coefficient. A method for evaluating the forced convection mean friction coefficient component, which may be used in estimating the power input required for maintaining the flow, has been proposed. [DOI: 10.1115/1.1373654]

Keywords: Conjugate, Finite Difference, Heat Transfer, Mixed Convection, Radiation

Introduction

Interaction of different modes of heat transfer continues to be a topic of interest because of its application in several areas, like the cooling of electronic equipment. Vertical board mounted electronic components are cooled by the removal of the heat generated in the components, with air as one of the promising cooling media. Zinnes [1] presented both numerical and experimental results of the problem of interaction of conduction with natural convection from a vertical plate with arbitrary surface heating, and showed that the degree of coupling between plate conduction and natural convection in the fluid is influenced by the plate-fluid thermal conductivity ratio. Gorski and Plumb [2] numerically investigated the problem of conjugate heat transfer from a single discrete heat source, flush-mounted in a flat plate. Here, the problem was solved using the well-known Blasius velocity profile for laminar forced convection as the input, and a correlation relating the average Nusselt number to Peclet number, the heat source size and the length ratio was developed. Hossain and Takhar [3] numerically investigated the effect of radiation on mixed convection from a heated vertical plate with uniform free-stream and surface temperatures. Cole [4] addressed, numerically, the problem of electronic cooling, from the perspective of scaling, applied to a steady viscous flow over a heated strip on a plate. However, the results for the problem of conjugate laminar mixed convection with surface radiation from a vertical plate with a flush-mounted discrete heat source are not available in the literature. Hence, a detailed numerical analysis of this problem is reported here.

Mathematical Formulation

The governing equations for two-dimensional, steady, incompressible, laminar, mixed convection from a vertical plate are available in a number of references, e.g., Bejan [5]. The schematic of the problem geometry, consisting of a vertical plate with a flush-mounted discrete heat source, is shown in Fig. 1. The left, top and bottom faces of the plate are insulated, while heat transfer occurs from the right face, by convection (free and forced) and surface radiation. The governing equations are first converted into vorticity-stream function (ω-ψ) form and are then normalized. As the present problem involves "conjugate" heat transfer, an "obvious" reference temperature difference does not exist. Hence, a "modified" reference temperature difference is introduced as $\Delta T_{\text{ref}}=(q_v L_h t/k_s)$. The normalized governing equations are

$$U\frac{d\omega}{\partial X}+V\frac{\partial\omega}{\partial Y}=-\text{Ri}_L^*\frac{\partial\theta}{\partial Y}+\frac{1}{\text{Re}_L}\left[\frac{\partial^2\omega}{\partial X^2}+\frac{\partial^2\omega}{\partial Y^2}\right] \tag{1}$$

$$\frac{\partial^2\psi}{\partial X^2}+\frac{\partial^2\psi}{\partial Y^2}=-\omega \tag{2}$$

$$U\frac{\partial\theta}{\partial X}+V\frac{\partial\theta}{\partial Y}=\frac{1}{\text{Pe}_L}\left[\frac{\partial^2\theta}{\partial X^2}+\frac{\partial^2\theta}{\partial Y^2}\right]. \tag{3}$$

Computational Domain

Based on an earlier work of the present authors, Gururaja Rao et al. [6], the computational domain in this case is extended beyond the trailing edge of the plate by a length equal to that of the plate (L), while the width (W) of the domain is taken equal to the plate length.

Boundary Conditions

At the bottom, as the fluid enters with a uniform velocity, u_∞, and temperature, T_∞, $(\partial\psi/\partial Y)=1$, $\omega=0$ and $\theta=0$. Along the plate, $\psi=0$ and $\omega=-\partial^2\psi/\partial Y^2$. Energy balance on the plate element, which is shown, enlarged, in the inset to Fig. 1, yields the following equation for the plate temperature distribution, in the non-dimensional form:

$$\frac{\partial^2\theta}{\partial X^2}+\gamma\left(\frac{\partial\theta}{\partial Y}\right)_{Y=0}+A_{r_1}A_{r_2}-\varepsilon\gamma N_{RF}\left[\left(\frac{T}{T_\infty}\right)^4-1\right]=0. \tag{4}$$

Equation (4) is valid in the region that contains the heat source. In the region outside the heat source, the term $A_{r_1}A_{r_2}=0$. Energy balance on the bottom and top insulated ends will give the appropriate equations, depending on whether or not these two ends are part of the heat source. With regard to the extended length of the left boundary, because of symmetry, $V=0$, which means that $(\partial\psi/\partial X)=0$, implying that ψ is a constant. Since $\psi=0$ has been taken along the plate, the same is used along the extended length

Contributed by the Heat Transfer Division for publication in the JOURNAL OF HEAT TRANSFER. Manuscript received by the Heat Transfer Division May 30, 2000; revision received November 25, 2000. Associate Editor: R. Skocypec.

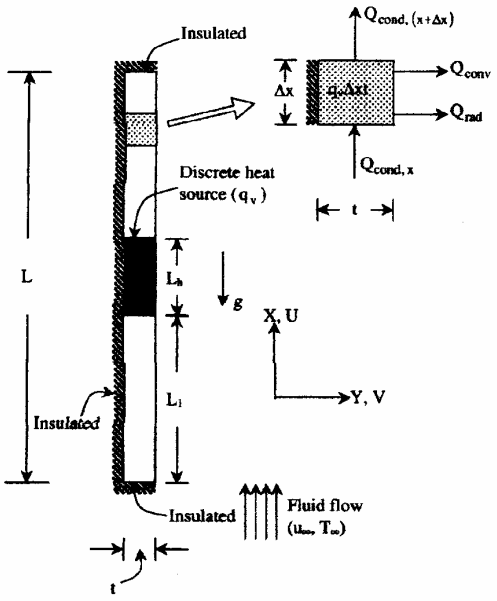

Fig. 1 Schematic of the problem geometry (inset showing an enlarged plate element)

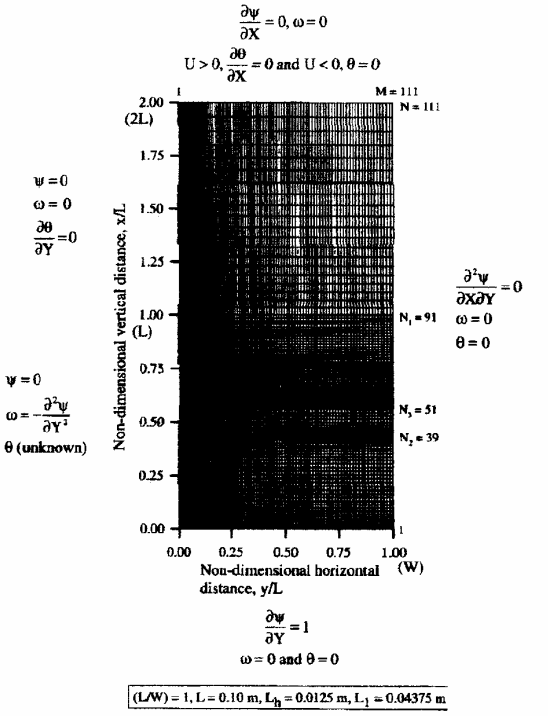

Fig. 2 Grid pattern used for a typical case along with boundary conditions

of the left boundary also. The vorticity, $\omega = 0$ here. Because there is no heat transfer across the extended length, $(\partial\theta/\partial Y) = 0$. On the top, the fully developed condition, $(\partial\psi/\partial X) = 0$, has been used for ψ. Since the domain is extended, $\omega = 0$. When U is positive, the fully developed condition $(\partial\theta/\partial X) = 0$ is used for θ, and when U is negative, $\theta = 0$. On the right, a mixed condition, $(\partial^2\psi/\partial X\partial Y) = 0$, is imposed on ψ, while ω and θ are each taken to be zero.

Method of Solution

The governing Eq. (1)–(3) are transformed into finite difference equations using a finite-volume based finite difference method of Gosman et al. [7] and are then solved using the Gauss-Seidel iterative procedure. The details of the solution procedure are available in Gururaja Rao et al. [6]. A hybrid grid system is used for discretizing the computational domain, keeping in mind the fact that the temperature distribution along the plate depends on the height and the position of the heat source. Based on a grid sensitivity test to be discussed in the ensuing section a grid size of 111×111 is chosen. The grid pattern used for a typical case is shown in Fig. 2, which also shows all the boundary conditions. All the calculations are done for air (Pr = 0.71) and the range of parameters used in the present work is listed in Table 1.

Results and Discussion

Grid Sensitivity Analysis. To study the effect of grid size $(M \times N)$ on the solution, a case with $q_v = 5 \times 10^5$ W/m^3, $A_1 = 0.4375$, $k_s = 0.25$ W/m K, $\varepsilon = 0.45$, $Re_L = 1275$, and $Ri_L^* = 2$ is considered, and the results are shown in Table 2. The analysis is made in two stages-first with M fixed and then with N fixed. The results of the former show that the difference in θ_{max} between grid sizes 111×111 and 111×131 is 0.06 percent, while the difference in $\bar{C}_f$ between the same grid sizes is 0.62 percent. The results of the grid sensitivity with N fixed show that the differences in θ_{max} and $\bar{C}_f$ between grid sizes 111×111 and 131×111 are 0.07 percent and 0.54 percent, respectively. In view of the above, M and N have both been fixed as 111. The nodal number 111 is considered as the basis after some initial studies with various other numbers.

Validation

The fundamental difference between the boundary conditions for laminar mixed convection from an isothermal vertical plate, e.g., Gururaja Rao et al. [6] and those used in the present work is the temperature variation along the plate. In the former, the temperature was considered uniform along the plate, while here, the temperature varies along the plate, provided with a heat source, due to multi-mode heat transfer. Thus, the validation of results for the entire mixed convection regime, provided in Gururaja Rao et al. [6] with reference to both numerical and experimental results available in the literature, will ensure the accuracy of the present results.

Table 1 Range of parameters [$L = 0.10$ m, $t = 0.0015$ m, $L_h = 0.0125$ m]

Parameter	Unit
$10^5 \le q_v \le 10^6$	W/m^3
$0 \le A_1 < 1$	-
$0.25 \le k_s \le 1$	W/m K
$0 < \gamma \le 10$	-
$0 < N_{RF} \le 1000$	-
$0.05 \le \varepsilon \le 0.85$	-
$80 \le Re_L \le 8000$	-
$0.1 \le Ri_L^* \le 25$	-

Table 2 Grid sensitivity analysis [$L=0.10$ m, $L_h=0.0125$ m, $t=0.0015$ m, $L_f=0.04375$ m, $q_v=5\times10^5$ W/m^3, $k_s=0.25$ W/m K, $\varepsilon=0.45$, $k_f=0.0291$ W/m K, $Re_L=1275$ and $Ri_L^*=2$]

Stage	Grid size (M×N)	θ_{max}	Percentage change (abs.)	$\overline{Cr}$ (total)	Percentage change (abs.)
(1) M = 111, N varied	111×91	1.0429	-	0.0642	-
	111×111	1.0348	0.78	0.0648	0.86
	111×131	1.0355	0.06	0.0644	0.62
(2) N = 111, M varied	91×111	1.0357	-	0.0652	-
	111×111	1.0348	0.09	0.0648	0.57
	131×111	1.0341	0.07	0.0644	0.54

The results of the present problem are also tested for mass and energy balance. For this, a typical case with $q_v=10^6$ W/m^3, $k_s=0.25$ W/m K, $\varepsilon=0.85$, $Re_L=2500$, and $Ri_L^*=1$ is taken up. As many as 13 different positions for the discrete heat source ($0\leq A_1\leq0.875$) are considered. The mass and the energy balance are found satisfactory within ± 0.007 percent and ± 4.02 percent, respectively.

Variation of Maximum Plate Temperature (θ_{max}) With Other Parameters

Figure 3 shows the variation of θ_{max} with non-dimensional heat source position (A_1), for two values of u_∞ ($Ri_L^*=25$ and 0.1) and two values of surface emissivity ($\varepsilon=0.05$ and 0.85), for the case with $q_v=10^6$ W/m^3 and $k_s=0.25$ W/m K. It is clear that there is a sharp increase in θ_{max} from $A_1=0$ to $A_1=0.125$ and again from $A_1=0.825$ to $A_1=0.875$, with a considerably slower increase for $A_1=0.125$ to 0.825. As Ri_L^* decreases from 25 to 0.1, the amount by which θ_{max} increases between the positions $A_1=0.125$ and $A_1=0.825$ also increases. In the case considered here, the increase in θ_{max}, between $A_1=0.125$ and $A_1=0.825$, for $Ri_L^*=25$ and $\varepsilon=0.85$, is only 2.8 percent, while that for $Ri_L^*=0.1$ is 14.4 percent. The θ_{max} decreases with increasing Re_L (or decreasing Ri_L^*), for a given A_1. The figure shows that the best position for the heat source is $A_1=0$ (leading edge of the plate), while the least advisable position is $A_1=0.875$ (heat source ending on the trailing edge) for all values of Ri_L^* and ε. For example, for $Ri_L^*=0.1$ and $\varepsilon=0.85$, θ_{max} increases by as much as 51 percent as the heat source shifts from $A_1=0$ to $A_1=0.875$. Further, θ_{max} decreases with increasing ε for a given Ri_L^*. The effect of ε on θ_{max} is more pronounced in the free convection dominant regime than in the forced convection dominant regime, which is consistent with the findings of earlier studies on natural convection-surface radiation interaction in enclosures, e.g., Dehghan and Behnia [8].

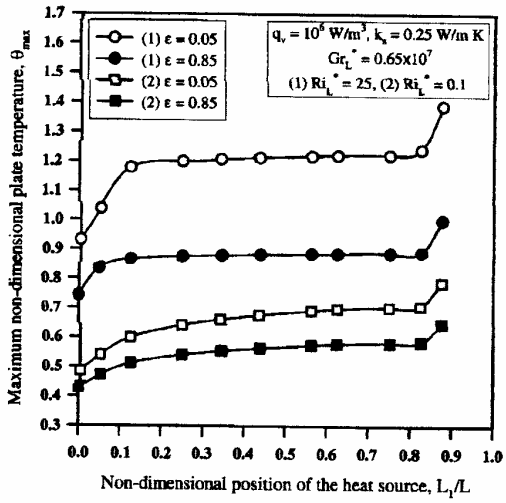

Fig. 3 Maximum non-dimensional plate temperature with modified Richardson number and surface emissivity for various positions of the discrete heat source

Heat Transfer Characteristics

Figure 4 shows the contributions of convection and radiation, plotted against A_1, for two values of Ri_L^* (25 and 0.1) and two values of ε (0.05 and 0.85), for the case with $q_v=10^6$ W/m^3, $k_s=0.25$ W/m K. A notable feature is the behavior of the two curves drawn for $Ri_L^*=25$ and $\varepsilon=0.85$. It is seen that the contribution of convection decreases from 45 percent for $A_1=0$ to about 41.5 percent for $A_1=0.05$, but from then increases monotonically to a maximum of 65 percent for $A_1=0.875$. An exact "mirror image" variation is noticed for radiation. The two curves cross each other for $A_1=0.625$, implying equal contributions from the two modes. The contribution from radiation decreases continuously from the free convection limit ($Ri_L^*=25$) to the forced convection limit ($Ri_L^*=0.1$), for a given ε. For $Ri_L^*=25$ and $\varepsilon=0.85$, radiation is significant with maximum and minimum contributions of 58.5 percent and 36 percent, respectively, depending on the position of the heat source. Even for $Ri_L^*=0.1$ (and the same $\varepsilon=0.85$), radiation plays a key role with maximum and minimum contributions of 30.5 percent and 18.3 percent, respectively. Convection is the dominant mode of heat transfer for a good reflecting surface ($\varepsilon=0.05$). For the case of the heat source located at the center of the plate, for $Ri_L^*=0.1$ and $\varepsilon=0.05$, convection takes away as much as 97.6 percent of the heat, while the radiation contribution is only 2.4 percent. The contribution from radiation increases with ε, with a proportionate decrease in convection. For $Ri_L^*=25$ and $A_1=0$, radiation contributes about 6.1 percent for $\varepsilon=0.05$, while, for $\varepsilon=0.85$, there is more than nine fold increase to 55.1 percent.

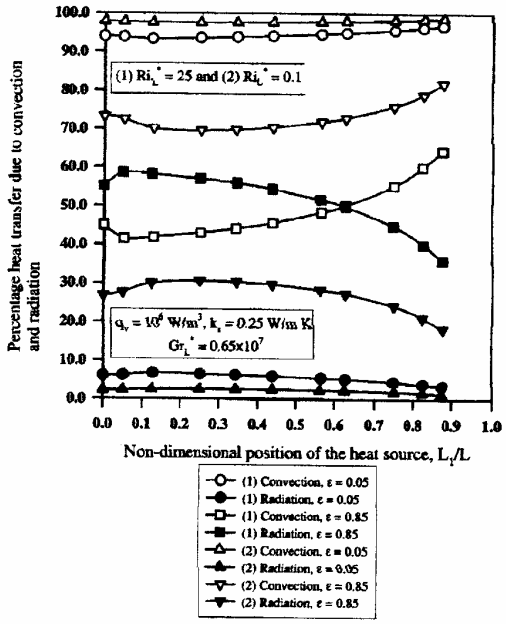

Fig. 4 Percentage heat transfer due to convection and radiation with modified Richardson number and surface emissivity for various positions of the discrete heat source

Effect of Thermal Conductivity of the Plate

The thermal conductivity of the plate (k_s) is present in ΔT_{ref}, which, in turn, is present in Gr_L^*, Ri_L^*, and N_{RF}. Thus, k_s alone cannot be varied by setting all the three dimensionless variables, Gr_L^*, Ri_L^*, and N_{RF}, for a given q_v. However, keeping all the primary variables fixed and letting k_s alone vary (0.25, 0.5, and 1 W/m K), the dimensional maximum plate temperature (T_{max}) is calculated for a representative case with $q_v = 10^6$ W/m^3, $u_\infty = 0.25$ m/s, $T_\infty = 25°C$ (298 K), $\varepsilon = 0.45$, and $A_1 = 0.4375$. It has been noticed that T_{max} decreases by 18.9 percent as k_s increases form 0.25 to 1 W/m K, in this particular case. This demonstrates the importance of k_s in the present problem.

Correlations

A correlation, having a correlation coefficient of 0.99 and an error band of ±5.8 percent, is evolved for θ_{max}, based on a large set of 514 data, as

$$\theta_{max} = 51.5181(1-A_1)^{-0.14}\gamma^{-0.69}\left(\frac{N_{RF}}{1+N_{RF}}\right)^{0.07}(1+\varepsilon)^{-0.51} \times (1+Ri_L^*)^{-0.139}\,Re_L^{-0.323}. \quad (5)$$

A correlation, having a correlation coefficient of 0.986 and an error band of ±6.1 percent, is developed for θ_{av} as

$$\theta_{av} = 54.4132(1-A_1)^{0.25}\gamma^{-0.89}\left(\frac{N_{RF}}{1+N_{RF}}\right)^{-1.91}(1+\varepsilon)^{-0.78} \times (1+Ri_L^*)^{-0.179}\,Re_L^{-0.415}. \quad (6)$$

Two separate correlations are generated for $\bar{C}_f$ for two different ranges of Ri_L^*, viz., $0.1 \le Ri_L^* \le 1$ and $1 < Ri_L^* \le 25$. The $\bar{C}_f$ for "low" modified Richardson number range ($0.1 \le Ri_L^* \le 1$), based on 245 data, having a correlation coefficient of 0.992 and an error band of ±4.6 percent, correlated as

$$\bar{C}_f = 6.8719(1-A_1)^{0.03}\gamma^{-0.08}\left(\frac{N_{RF}}{1+N_{RF}}\right)^{-0.8}(1+\varepsilon)^{-0.05} \times (1+Ri_L^*)^{0.239}\,Re_L^{-0.672}. \quad (7)$$

The correlation for $\bar{C}_f$ for "high" modified Richardson number range ($1 < Ri_L^* \le 25$), based on 196 data, having a correlation coefficient of 0.99 and an error band of ±5.4 percent, came out as

$$\bar{C}_f = 38.155(1-A_1)^{0.39}\gamma^{-0.47}\left(\frac{N_{RF}}{1+N_{RF}}\right)^{-0.25}(1+\varepsilon)^{-0.54} \times (1+Ri_L^*)^{0.493}\,Re_L^{-0.792}. \quad (8)$$

Calculation of Forced Convection Friction Coefficient Component

Equations (7) and (8) give the sum of the free and forced convection components of the mean friction coefficient. Of these, only the forced convection component requires the power input (pumping power), through a fan or blower, for maintaining the flow. The free convection related flow, results from buoyancy, and hence does not need any power input. Now, the point of interest is to obtain $\bar{C}_f$ (forced) from the correlations for the total $\bar{C}_f$ evolved above. For this, the present problem is solved for two typical cases, for as many as eight values of Ri_L^* covering the entire range $0.1 \le Ri_L^* \le 25$ in each case. The problem is solved first as such and later with $\beta = 0$ (no free convection), which, respectively, gave the values of $\bar{C}_f$ (total) and $\bar{C}_f$ (forced). From these, the values of $\bar{C}_f$ (free) are obtained. The percentages of the two components are plotted against Ri_L^*, for both the cases, as shown in Fig. 5, which reveals that $Ri_L^* = 0.1$ and 25 could be taken as the forced and free convection limits, respectively, with pure mixed

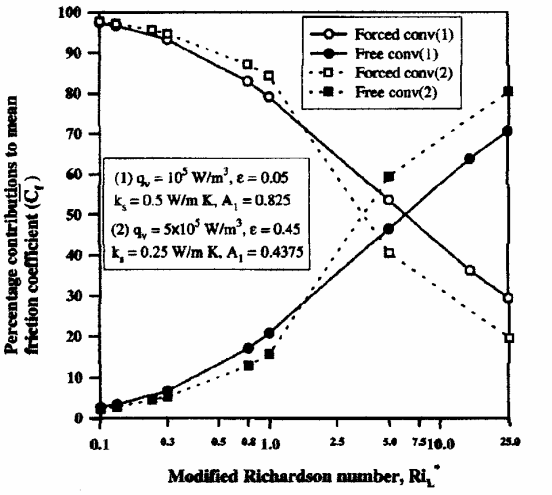

Fig. 5 Percentage contributions to mean friction coefficient from forced and free convection components

convection falling in the range $1 \le Ri_L^* \le 10$. In view of this, it has been decided to check whether $0.1 \le Ri_L^* \le 1$ would serve as the forced convection asymptote. To do this, 26 randomly chosen data, covering the entire range ($0.1 \le Ri_L^* \le 25$), are generated with $\beta = 0$ (no free convection). The values of $\bar{C}_f$ (forced), thus obtained, are compared with the values of $\bar{C}_f$ obtained by letting $Ri_L^* = 0$ in Eq. (7), and a very good agreement, with an error band of ±6.3 percent, is noticed. Therefore, $\bar{C}_f$ (forced) for the whole range of Ri_L^* ($0.1 \le Ri_L^* \le 25$) may be obtained from Eq. (7), by simply setting $Ri_L^* = 0$, as

$$\bar{C}_f(\text{forced}) = 6.8719(1-A_1)^{0.03}\gamma^{-0.08}\left(\frac{N_{RF}}{1+N_{RF}}\right)^{-0.8} \times (1+\varepsilon)^{-0.05}\,Re_L^{-0.672}. \quad (9)$$

From the $\bar{C}_f$ (forced), the wall shear, the drag force and thus the fan power input may be calculated.

Conclusions

The best position for the heat source is the leading edge of the plate and the least preferable position is the trailing edge, as the latter position increases θ_{max} by 35–50 percent for the entire range of Ri_L^*. The θ_{max}, for the given values of q_v and k_s, decreases with ε for any given Re_L or Ri_L^*. However, the degree of decrease of θ_{max} with ε decreases, as one moves from the free convection limit ($Ri_L^* = 25$) to the forced convection limit ($Ri_L^* = 0.1$). Radiation is found to play a significant role in the present problem. For example, for $\varepsilon = 0.85$, for $Ri_L^* = 25$, radiation is found to contribute 35–60 percent of heat transfer, depending on the position of the heat source. While, for the same $\varepsilon = 0.85$, for $Ri_L^* = 1$ and 0.1, the radiation contributions have been found to be 28–45 percent and 18–30 percent, respectively. For a given Ri_L^* (say for $Ri_L^* \sim 1$), convection is dominant, taking away as much as 90–95 percent of the heat generated, in the case of a good reflecting surface ($\varepsilon = 0.05$), with radiation being insignificant. However, the radiation contribution increases with ε for the same Ri_L^* and it may be as high as 45–50 percent, in the case of a good emitting surface ($\varepsilon = 0.85$). Correlations are developed for θ_{max} and θ_{av} along with two separate correlations for $\bar{C}_f$ for two different

ranges of Ri_L^*. A method for evaluating the forced convection friction coefficient component is provided, which helps in the estimation of the fan or blower power input required for maintaining the flow.

Nomenclature

A_1 = non-dimensional position of the heat source, (L_1/L)
A_{r_1}, A_{r_2} = aspect ratios pertaining to problem geometry, (L/t), (L/L_h), respectively
$\bar{C}_f$ = mean friction coefficient, $(2/\mathrm{Re}_L)\int_0^1 (\partial U/\partial Y)_{Y=0} dX$
Gr_L^* = modified Grashof number based on L, $g\beta\Delta T_{\mathrm{ref}} L^3/\nu^2$
g = acceleration due to gravity, 9.81 m/s^2
H, W = height and width of the computational domain, respectively, m
k = thermal conductivity, W/m K
L, t = length and thickness of the vertical plate, respectively, m
L_h, L_1 = height and starting length of the discrete heat source, respectively, m
M, N = number of grid points in horizontal and vertical directions, respectively
N_{RF} = radiation-flow interaction parameter, $\sigma T_\infty^4 \Delta T_{\mathrm{ref}}/(k_f/L)$
P = pressure at any location, Pa
Pe_L = Peclet number based on L, $u_\infty L/\alpha$
q_v = volumetric heat generation rate in the discrete heat source, W/m^3
Q = heat transfer rate, W
Re_L = Reynolds number based on L, $u_\infty L/\nu$
Ri_L^* = modified Richardson number based on L, $(\mathrm{Gr}_L^*/\mathrm{Re}_L^2)$ or $g\beta\Delta T_{\mathrm{ref}} L/u_\infty^2$
T = temperature at any location, K
u_∞ = free-stream velocity of the fluid, m/s
u = vertical velocity, m/s
U = non-dimensional vertical velocity, u/u_∞ or $\partial\psi/\partial Y$
v = horizontal velocity, m/s
V = non-dimensional horizontal velocity, v/u_∞ or $-\partial\psi/\partial X$
x, y = vertical and horizontal distances, respectively, m
X, Y = non-dimensional vertical and horizontal distances, $x/L, y/L$, respectively
α = thermal diffusivity of the fluid, m^2/s
β = isobaric cubic expansivity of the fluid, $-(1/\rho)\times(\partial\rho/\partial T)_P, K^{-1}$
ΔT_{ref} = modified reference temperature difference, $q_v L_h t/k_s, K$
Δx = height of the plate element, m
ΔX = non-dimensional height of the plate element, $\Delta x/L$
ε = emissivity of the plate surface
δ = convergence criterion in percentage form, $|(\zeta_{\mathrm{new}} - \zeta_{\mathrm{old}})/\zeta_{\mathrm{new}}| \times 100$ percent
γ = non-dimensional thermal conductivity parameter, $k_f L/k_s t$
ν = kinematic viscosity of the fluid, m^2/s
ω' = vorticity, s^{-1}
ω = non-dimensional vorticity, $\omega' L/u_\infty$
ρ = density of the fluid, kg/m^3
σ = Stefan-Boltzmann constant, 5.6697×10^{-8} W/m^2 K^4
ψ' = stream function, m^2/s
ψ = non-dimensional stream function, $\psi'/u_\infty L$
θ = non-dimensional temperature, $(T-T_\infty)/\Delta T_{\mathrm{ref}}$
ζ = dependent variable (ψ, ω, or θ) over which convergence test is applied

Subscripts

av, max, p = average, maximum and local values of the plate temperature, respectively
f, s = fluid and plate material, respectively
new, old = values of the dependent variable from present and previous iterations, respectively

References

[1] Zinnes, A. E., 1970, "The Coupling of Conduction with Laminar Natural Convection From a Vertical Flat Plate With Arbitrary Surface Heating," ASME Journal of Heat Transfer, **92**, pp. 528–534.
[2] Gorski, M. A., and Plumb, O. A., 1992, "Conjugate Heat Transfer from an Isolated Heat Source in a Plane Wall," Proc. Winter Annual Meeting of The American Society of Mechanical Engineers, ASME HTD-210, pp. 99–105.
[3] Hossain, M. A., and Takhar, H. S., 1996, "Radiation Effect on Mixed Convection Along a Vertical Plate with Uniform Surface Temperature," Heat and Mass Transfer/Warme-und Stoffubertragung, **31**, pp. 243–248.
[4] Cole, K. D., 1997, "Conjugate Heat Transfer from a Small Heated Strip," Int. J. Heat Mass Transf., **40**, pp. 2709–2719.
[5] Bejan, A., 1984, *Convection Heat Transfer*, Wiley, New York, pp. 112–114.
[6] Gururaja Rao, C., Balaji, C., and Venkateshan, S. P., 2000, "Numerical Study of Laminar Mixed Convection from a Vertical Plate," I. J. Trans. Phenomena, **2**, pp. 143–157.
[7] Gosman, A. D., Pun, W. M., Runchal, A. K., Spalding, D. B., and Wolfshtein, M., 1969, *Heat and Mass Transfer in Recirculating Flows*, Academic Press, London, pp. 89–137.
[8] Dehghan, A. A., and Behnia, M., 1996, "Combined Natural Convection—Conduction and Radiation Heat Transfer in a Discretely Heated Open Cavity," ASME Journal of Heat Transfer, **118**, pp. 56–64.